M. Tokarev *
(on behalf of the STAR Collaboration)

RECENT **STAR** SPIN RESULTS
AND SPIN MEASUREMENTS AT **RHIC**

* E-mail: tokarev@jinr.ru

Токарев М. (от имени коллаборации STAR) E1-2018-11

Последние результаты коллаборации STAR по спиновой физике на RHIC

Коллаборация STAR проводит измерения одно- и двухспиновых асимметрий в столкновениях продольно- и поперечно-поляризованных протонов при энергии $\sqrt{s} = 200$ и 510 ГэВ для более глубокого изучения структуры спина протона и динамики партонных взаимодействий в широком диапазоне энергии столкновения, импульсов и быстрот различных рождающихся пробников. Изучение процессов с рождением $W^{\pm}$-бозонов позволяет получить информацию о спин-зависимой флейворной структуре спина протона. Представлен обзор последних результатов STAR по измерению двойной продольной асимметрии (A_{LL}) рождения пионов и струй при энергии $\sqrt{s} = 200$ и 510 ГэВ, одиночной продольной (A_L) и поперечной (A_N) асимметрий рождения $W^{\pm}$-бозонов при $\sqrt{s} = 510$ ГэВ. Обсуждаются результаты STAR по одиночной поперечной азимутальной асимметрии рождения пионов в $p^{\uparrow} + (p,\ \text{Au})$- и jet $+\ \pi^{\pm}$ в $p^{\uparrow} + p$-столкновениях. Включение новых детекторных систем — Forward Calorimeter System (FCS) и Forward Tracking System (FTS) — значительно улучшит возможности установки STAR для измерения асимметрий рождения пионов, струй и дрелл-яновских пар в области больших быстрот.

Tokarev M. (on behalf of the STAR Collaboration) E1-2018-11

Recent STAR Spin Results and Spin Measurements at RHIC

The STAR experiment provides measurements of single- and double-spin asymmetries in longitudinally and transversely polarized $p + p$ collisions at $\sqrt{s} = 200$ and 510 GeV to deepen our understanding of the proton spin structure and dynamics of parton interactions over a wide range of collision energy, momentum and rapidity of the various produced probes. Polarized processes with $W^{\pm}$ production allow us to study the spin-flavor structure of the proton. Recent results obtained by STAR on the double longitudinal asymmetry, A_{LL}, of pion and jet production at $\sqrt{s} = 200$ and 510 GeV, the single longitudinal, A_L, and transverse, A_N, asymmetry of $W^{\pm}$ production at $\sqrt{s} = 510$ GeV are overviewed. STAR results on azimuthal single transverse asymmetry of pion in $p^{\uparrow} + (p,\ \text{Au})$ and jet $+\ \pi^{\pm}$ in $p^{\uparrow} + p$ collisions are discussed. The proposed Forward Calorimeter System (FCS) and Forward Tracking System (FTS) upgrades at STAR would significantly improve the capabilities of existing detectors for measurements of observables such as asymmetries of pion, jet, Drell–Yan pairs produced at forward rapidities.

1. INTRODUCTION

The Relativistic Heavy Ion Collider (RHIC) located at the Brookhaven National Laboratory was built to collide heavy ions at center-of-mass energies of up to 200 GeV per colliding nucleon pair and polarized protons at center-of-mass energies ranging from 50 to 500 GeV [1]. The RHIC storage ring is 3.83 km in circumference and is designed with six interaction points (IPs) at which beam collisions are possible. There are a total of 120 possible bunches, typically 109–111 are filled. The time between bunch crossings at the IPs is 106 ns. Polarizations of up to 65% for 100 GeV proton beams and about 60% for 255 GeV beams have been achieved. The maximum luminosities achieved thus far are $1.2 \cdot 10^{32}$ cm$^{-2} \cdot$ s^{-1} at $\sqrt{s} = 200$ GeV and $2.5 \cdot 10^{32}$ cm$^{-2} \cdot$ s^{-1} at $\sqrt{s} = 510$ GeV. RHIC is the first and only high-energy polarized proton–proton collider in the world [2]. The BNL hadron facility complex including the AGS Booster, the AGS, and RHIC is shown in Fig. 1. In the case of polarized proton running at RHIC, a pulse of polarized H$^-$ ions from the source is accelerated to 200 MeV in the linac, then stripped of its electrons as it is injected and captured as a single bunch of polarized protons in the Booster, which accelerates the protons to 1.5 GeV. The bunch of polarized protons is then transferred to the Alternating Gradient Synchrotron (AGS) and accelerated to 24 GeV before injection into RHIC. Each bunch is accelerated in the AGS and injected into RHIC independently, with the two RHIC rings being filled one bunch at a time. The direction of the polarization vector is selected for each bunch separately. The nominal fill duration is 8 h, after which the beams are dumped and fresh beams are injected into RHIC. The bunch-by-bunch polarization patterns in consecutive fills are varied in order to reduce potential systematic effects. Polarized proton injection uses an optically pumped polarized H$^-$ ion source [3]. H$^-$ polarization at the source of 85% has been achieved. Siberian snakes [4], a series of spin-rotating dipoles, are used to overcome both imperfection and intrinsic depolarizing resonances in RHIC. The two snakes installed in each RHIC ring rotate the spin vector $180°$ about horizontal axes. To provide full-energy polarized beams, the polarization has been measured at various stages of acceleration in order to identify and address possible origins of depolarization at each step. There are two types of polarimeters installed in RHIC. The fast proton–carbon (pC) polarimeter [5] takes advantage of a known analyzing power $A_N^{p\mathrm{C}} \simeq 0.01$ in the elastic scattering of polarized protons with carbon atoms which originates from
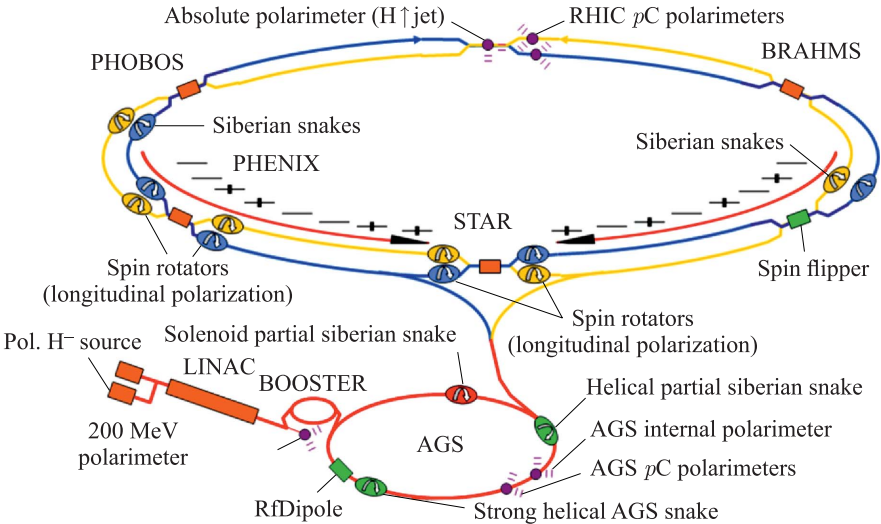
1

Fig. 1. Polarized $p + p$ collider at BNL [2]

interference between electromagnetic and hadronic elastic scattering amplitudes. The pC polarimeter can make measurement in a few (1–2) seconds and provide immediate information on the stability of the beam polarization from a few data points taken over the several hours of a fill.

Calibration of the pC polarimeter to an absolute beam polarization uncertainty of less than 5% can then be provided by measuring polarized elastic $p+p$ scattering with a polarized hydrogen-jet-target polarimeter [6]. The hydrogen-jet-target polarization reaches greater than 90% with accuracy about 3% in absolute value.

The stable spin direction through acceleration and storage in RHIC is transverse to the protons momentum, in the vertical direction. Spin rotator dipole magnets have been used to achieve both radial and longitudinal spin [7]. The rotators are located outside the interaction regions of the PHENIX and STAR experiments.

2. STAR DETECTOR

The main detectors of the STAR experiment (Fig. 2) [8] used to obtain the results on p_T spectra, yields, and particle ratios for charged hadrons are the Time Projection Chamber (TPC) [9] and Time-of-Flight detectors (ToF) [10]. The TPC is the primary tracking device at STAR. It is 4.2 m long and 4 m in diameter. Its uniform acceptance covers about ± 1 units of pseudorapidity (η) and the full azimuthal angle. TPC is placed in the uniform solenoidal magnetic field (0.5 T). The sensitive volume of the TPC contains P10 gas (10% methane, 90% argon) regulated at 2 mbar above atmospheric pressure. The TPC data
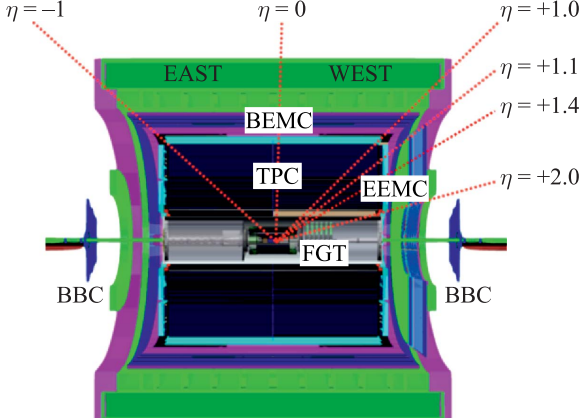
2

Fig. 2. STAR detector [8]

are used to determine particle trajectories, momenta, and particle type through ionization energy loss (dE/dx). The ToF is based on Multi-Gap Resistive Plate Chamber (MRPC) technology and is very useful to identify the particles in a relatively higher momentum range compared to TPC. The Multi-Gap Resistive Plate Chamber Time of Flight (MRPC ToF) [11,12] surrounds the outer radius of the TPC, $|\eta| < 0.9$, $0 < \phi < 2\pi$. It consists of 23 K channels from 120 modules. The details of the design and other characteristics of the STAR detectors can be found in [8].

The STAR detector subsystems used to reconstruct jets are the TPC and the barrel and endcap electromagnetic calorimeters (BEMC, EEMC) [13, 14].

The TPC provides charged-particle tracking in a 0.5 T solenoidal magnetic field over the range $|\eta| < 1.3$ in pseudorapidity and 2π in azimuthal angle ϕ. The BEMC and EEMC are segmented lead-scintillator sampling calorimeters, which provide full azimuthal coverage $|\eta| < 1$ and $1.09 < \eta < 2$, respectively. The calorimeters measure electromagnetic energy deposition and provide the primary triggering information via fixed jet patches. Details of the track momentum and calorimeter energy resolutions can be found in [15]. The beam–beam counters (BBCs) [16] were used in the determination of the integrated luminosity and, along with the zero-degree calorimeters (ZDCs) [17] and vertex position detectors (VPDs) [18], in the determination of helicity-dependent relative luminosities.

3. ASYMMETRY A_{LL} OF JET PRODUCTION IN $\vec{p} + \vec{p}$ COLLISIONS AT 510 GeV

The quark–gluon and gluon–gluon scattering cross sections are very sensitive to the longitudinal helicities of the participating partons, so the inclusive jet longitudinal double-spin asymmetry, A_{LL}, provides direct sensitivity to the gluon

polarization in the proton. The asymmetry A_{LL} is defined as

$$A_{LL} = \frac{\sigma^{++} + \sigma^{--} - \sigma^{+-} - \sigma^{-+}}{\sigma^{++} + \sigma^{--} + \sigma^{+-} + \sigma^{-+}}, \qquad (1)$$

where σ^{++}, σ^{--} and σ^{+-}, σ^{-+} are the differential cross sections when both polarized beam protons have the same $(++, --)$ and opposite $(+-, -+)$ positive $(+)$ or negative $(-)$ helicities.

The data for A_{LL} recorded by STAR in 2009 were extracted from an integrated luminosity of 20 pb^{-1}. The successful measurements of A_{LL} during 2012 and 2013 runs have been performed at $\sqrt{s} = 510$ GeV with mean polarization 52% and 53%, respectively.

Figure 3 shows the longitudinal double-spin asymmetry, A_{LL}, for midrapidity inclusive jet production in polarized $\vec{p} + \vec{p}$ collisions at a center-of-mass energy of $\sqrt{s} = 200$ GeV (*a*) [19] and preliminary results at highest energy $\sqrt{s} =$

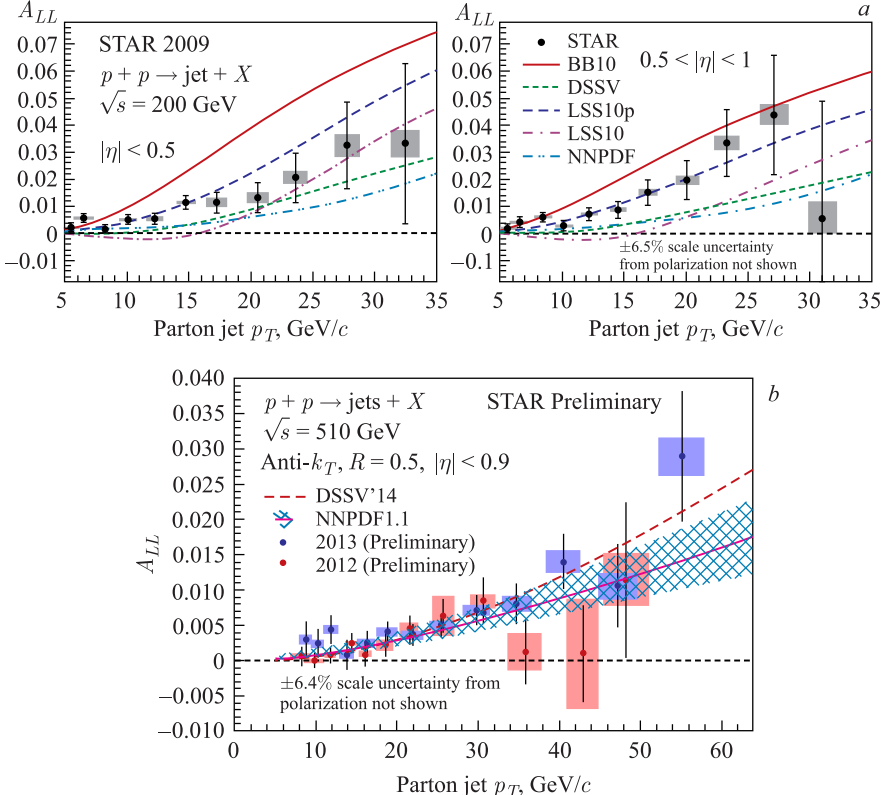Fig. 3. The longitudinal double-spin asymmetry, A_{LL}, of inclusive jet production in $\vec{p} + \vec{p}$ collisions at $\sqrt{s} = 200$ GeV (*a*) [19] and 510 GeV (*b*) [20] measured by STAR

510 GeV (*b*) [20]. According to the NNPDF group, the integral of ΔG over $0.05 < x < 0.5$ in NNPDFpol1.1 is 0.23 ± 0.07 [21]. The STAR data taken in 2009 run and included in updated global analyses provide evidence at the 3σ level for positive gluon polarization in the region $x > 0.05$. As seen from Fig. 3, *b*, A_{LL} at $\sqrt{s} = 510$ GeV is well described by global fits that previously gave a good description of the 2009 measurements at $\sqrt{s} = 200$ GeV as well.

4. ASYMMETRY A_{LL} OF DIJET PRODUCTION IN $\vec{p} + \vec{p}$ COLLISIONS AT 200 GeV

The dijet asymmetry A_{LL} represents an important advance in the experimental investigation of the gluon polarization and is the basis for future high statistics dijet measurements at STAR. Correlation measurements capture a more complete picture of the hard scattering kinematics and therefore offer better determination of the gluon momentum fraction than is possible with inclusive jet measurements. This improvement in x resolution will allow global analyses to constrain better the behavior of $\Delta g(x)$ as a function of x and the integrated value of $\Delta g(x)$.

Figure 4 presents the first measurement of the dijet cross section and the longitudinal double-spin asymmetry, A_{LL}, for midrapidity dijet production in polarized $\vec{p} + \vec{p}$ collisions at a center-of-mass energy of $\sqrt{s} = 200$ GeV [22]. The dijet cross section, as seen from Fig. 4, *a*, is consistent with next-to-leading order (NLO) perturbative QCD predictions [23, 24]. The theoretical cross section was corrected for underlying event and hadronization (UEH) effects. The UEH correction was estimated from simulation by taking the ratio of the particle-level over parton-level dijet yields. The ratio ranges from 1.44 at low mass to 1.22 at high mass. The systematic uncertainty on both the UEH correction and the theoretical cross section itself took into account the uncertainty on the PDF set used as well as sensitivity to the variation of the factorization and renormalization scales. The factorization and renormalization scales were varied independently, but the resulting deviation was always less than the simultaneous case. Dijet A_{LL} measurement for the same-sign (top) and opposite-sign (bottom) topological configurations as a function of dijet invariant mass is shown in Fig. 4, *b*. The asymmetry A_{LL} is presented for two distinct topologies: "same-sign" in which both jets have either positive or negative pseudorapidity, and "opposite-sign" in which one jet has positive and the other negative pseudorapidity. The opposite-sign topology selects events arising from relatively symmetric (in x) partonic collisions, whereas same-sign events select more asymmetric collisions. The most asymmetric, high-p_T collisions are preferentially between a high momentum (high x and therefore highly polarized) quark and a low momentum gluon. As seen from Fig. 4, *b*, the A_{LL} results are in reasonable agreement with predictions from several recent NLO global analyses [21, 25]. These first such correlation measurements support those analyses that find positive gluon polarization at the level of roughly 0.2 over the region of Bjorken-$x > 0.05$.
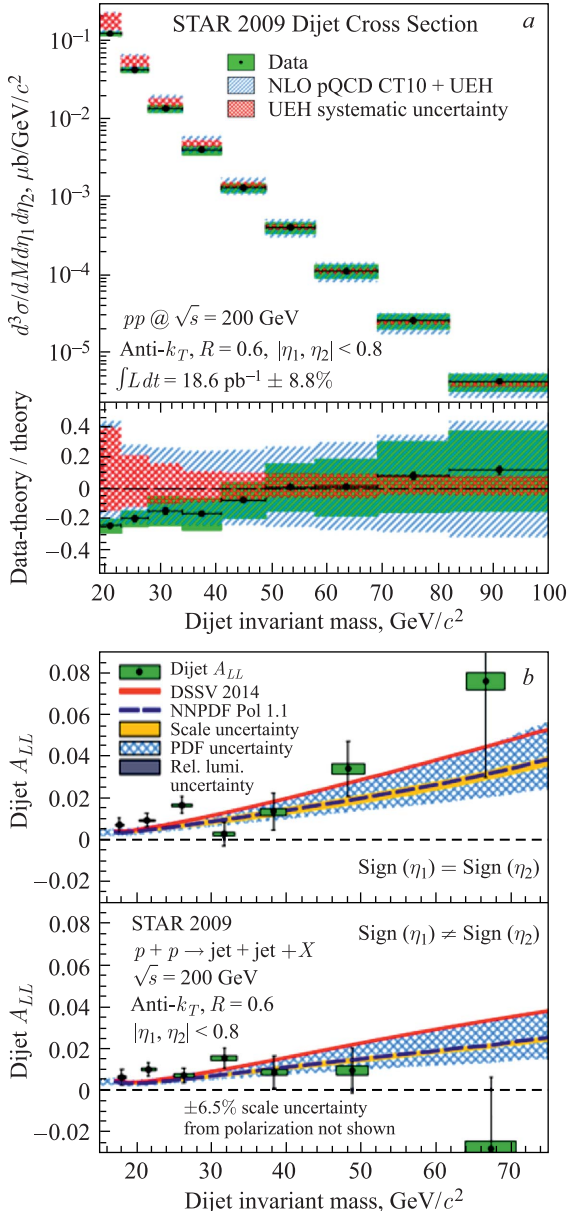
Fig. 4. The dijet differential cross section (*a*) and dijet asymmetry A_{LL} (*b*) for two topologies as a function of invariant mass measured by the STAR experiment [22]

6

5. ASYMMETRY A_L OF $W^{\pm}$ PRODUCTION
IN $\vec{p} + p$ COLLISIONS AT 510 GeV

The STAR experiment is well equipped to measure the single longitudinal asymmetry, A_L, for $W^{\pm}$-boson production within a pseudorapidity range of $|\eta| < 1$. The asymmetry A_L is defined as

$$A_L = \frac{\sigma^+ - \sigma^-}{\sigma^+ + \sigma^-}, \qquad (2)$$

where $\sigma^+(\sigma^-)$ is the differential cross section when polarized beam proton has the positive (negative) helicities. $W^{\pm}$ bosons are detected via their $W^{\pm} \to e^{\pm}\nu$ decay channels. A subsystem of the STAR detector, the Time Projection Chamber, is used to measure the transverse momentum (p_T) of decay electrons and positrons and to separate their charge sign. Two other subsystems, Barrel and Endcap Electromagnetic Calorimeters, are used to measure the energy of decay leptons and other particles. A well developed algorithm [26] is used to identify and reconstruct $W^{\pm}$ candidate events by removing QCD type background events.

The production of $W^{\pm}$ bosons in longitudinally polarized $\vec{p} + p$ collisions at RHIC provides a unique and powerful tool to probe the individual helicity PDFs of light quarks (Δu, Δd) and antiquarks ($\Delta \bar{u}$, $\Delta \bar{d}$) at large Q^2 scale. These distributions can be extracted by measuring the parity-violating asymmetry, A_L, as a function of the decay electron (positron) pseudorapidity, η_e. At leading order, $A_L^{W^+}$ is directly related to polarized anti-d and u quark distributions ($\Delta \bar{d}$, Δu), while $A_L^{W^-}$ is directly related to polarized anti-u and d quark distributions ($\Delta \bar{u}$, Δd) [27].

In [26] measurements of single- and double-spin asymmetries for weak boson production in longitudinally polarized $\vec{p} + p$ collisions from 2011 and 2012 by the STAR collaboration at RHIC for $\sqrt{s} = 510$ GeV are presented. The integrated luminosities of the data sets from 2011 and 2012 are 9 and 77 pb^{-1}, respectively. The data presented here for A_L^W were collected by the STAR experiment in RHIC 2013 running of longitudinally polarized $p + p$ collisions at $\sqrt{s} = 510$ GeV [28]. The total integrated luminosity of the data is 246.2 pb^{-1}, with an average beam polarization of 54%.

Figure 5 shows the longitudinal single-spin asymmetry, A_L, for $W^{\pm}$ production as a function of lepton pseudorapidity (η_e) in comparison to theory predictions [26, 28]. The measurement of the asymmetry in the rapidity region $1 < \eta < 1.4$ used STAR EEMC subsystem. As seen from Fig. 5, b, new preliminary 2013 results cover both the middle and forward rapidity ranges. They are consistent with previous STAR results based on the data collected during RHIC 2011 and 2012 runs and show a preference for a sizable, positive up antiquark polarization in the range $0.05 < x < 0.2$. The STAR 2013 new A_L^W results
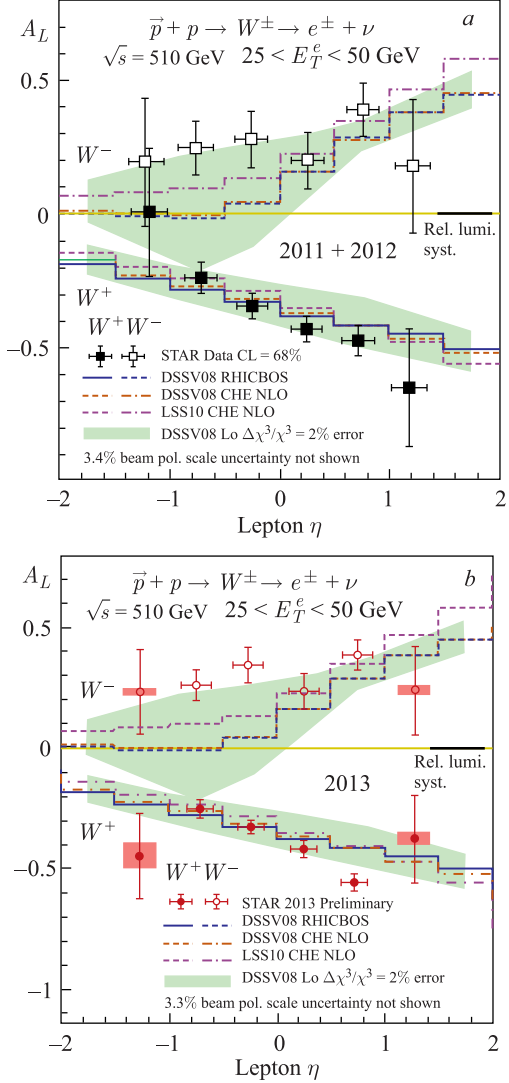
Fig. 5. The longitudinal single-spin asymmetry, A_L, of $W^{\pm}$ production in $\vec{p}+p$ collisions at $\sqrt{s} = 510$ GeV as a function of electron pseudorapidity η_e collected during RHIC 2011, 2012 (*a*) [26] and 2013 (*b*) [28] runs

have reached unprecedented precision and can be considered as the most precise measurements of A_L^W in the world to date. These will provide further constraints on light sea quark polarization and significantly advance our understanding of nucleon spin structure.

6. ASYMMETRY A_N OF $W^\pm$ PRODUCTION
IN $p^\uparrow + p$ COLLISIONS AT 500 GeV

The transverse single-spin asymmetry of weak boson production in transversely polarized proton–proton collisions at $\sqrt{s} = 500$ GeV with a recorded luminosity of 25 pb^{-1} by the STAR experiment at RHIC is presented in [29]. The asymmetry A_N is defined as

$$A_N = \frac{d\sigma^\uparrow - d\sigma^\downarrow}{d\sigma^\uparrow + d\sigma^\downarrow}, \tag{3}$$

where $d\sigma^\uparrow(d\sigma^\downarrow)$ is the differential cross section as a function of azimuthal angle with the spin direction of the proton beam pointing up (down).

The measured observable is sensitive to the Sivers function [30, 31], one of the transverse-momentum-dependent (TMD) parton distribution functions, which is predicted to have the opposite sign in proton–proton collisions to that observed in deep inelastic lepton–proton scattering (SIDIS). The Sivers function describes the correlation between the intrinsic transverse momentum of a parton and the spin of the parent proton. These data provide the first experimental investigation of the nonuniversality of the Sivers function, fundamental to our understanding of QCD.

Figure 6 shows a combined fit on W^+ and W^- asymmetry A_N [29] as a function of rapidity y^W to the theoretical prediction in the model [32] without
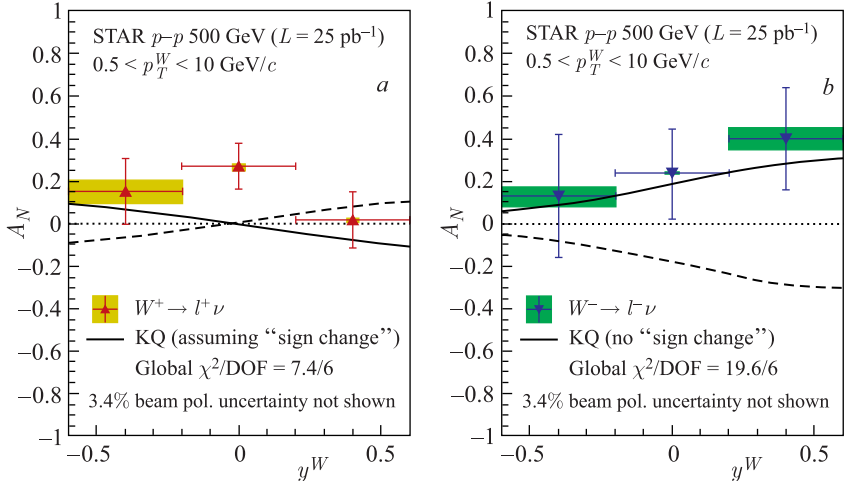

Fig. 6. The transverse single-spin asymmetry, A_N, of W^+ (a) and W^- (b) production in $p^\uparrow + p$ collisions at $\sqrt{s} = 500$ GeV [29]. The non-TMD evolved [32] model calculations assuming or excluding a sign change in the Sivers function are shown by solid and dashed lines, respectively

TMD evolution assuming a sign change in the Sivers function (the solid line) and without sign change (the dashed line). The current data favor theoretical models that include a change of sign for the Sivers function relative to observations in SIDIS measurements, if TMD evolution effects are small. The results presented here can help to constrain theoretical models including the TMD evolution [33–35].

7. ASYMMETRY A_N OF π^0 MESON PRODUCTION IN $p^\uparrow + p$ COLLISIONS AT $\sqrt{s} = 500$ GeV

The study of the transverse single-spin asymmetry, A_N, is also strongly related to our understanding of the structure of hadrons and their spin content in terms of partons (see [36] and references therein). In this sense they play a crucial role in the 3D mapping of the nucleons. The measurement of A_N in polarized $p^\uparrow + p$ collisions provides critical information on the higher-twist effects and transverse-momentum-dependent phenomena in parton distributions and fragmentation processes [37]. Various underlying mechanisms can contribute and need to be disentangled to understand the experimental observations in detail, in particular, the p_T-dependence. Among them are Sivers/Qiu–Sterman and Collins mechanisms. Understanding of these mechanisms will help to separate the contributions from initial and final states, and will give insight into the transverse spin structure of hadrons. The Sivers function describes the correlation of parton transverse momentum with the transverse spin of the nucleon. A non-vanishing correlation means that the Sivers function is azimuthally asymmetric in the transverse momentum space relative to the spin direction of the nucleon. The Collins function describes a correlation of the transverse spin of a scattered quark and
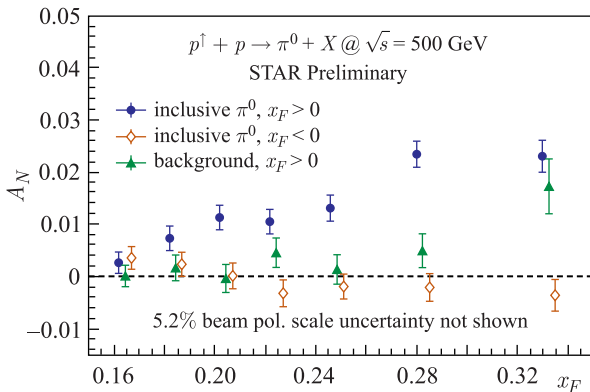

Fig. 7. The transverse single-spin asymmetry, A_N, of π^0 meson production in $p^\uparrow + p$ collisions at $\sqrt{s} = 500$ GeV [38]

the transverse momenta of the fragmentation products and as such can lead to an asymmetry of the distribution of hadrons in jets. Contrary to the Sivers effect, the Collins fragmentation function is assumed to be universal among different processes (SIDIS, e^+e^- annihilation, and $p + p$ collisions).

Figure 7 demonstrates the single-spin asymmetry in inclusive π^0 mesons detected within $2.8 < \eta < 4.0$ in proton–proton collisions measured by STAR at RHIC for the highest center-of-mass energies to date, $\sqrt{s} = 500$ GeV, as a function of Feynman-x_F. The measurements are based on the data taken in 2011 with integrated luminosity 22 pb^{-1} [38]. As seen from Fig. 7, the asymmetry A_N increases with x_F in the fragmentation range of polarized proton ($x_F > 0$). A similar trend is observed at lower energies [39–41]. Asymmetry is consistent
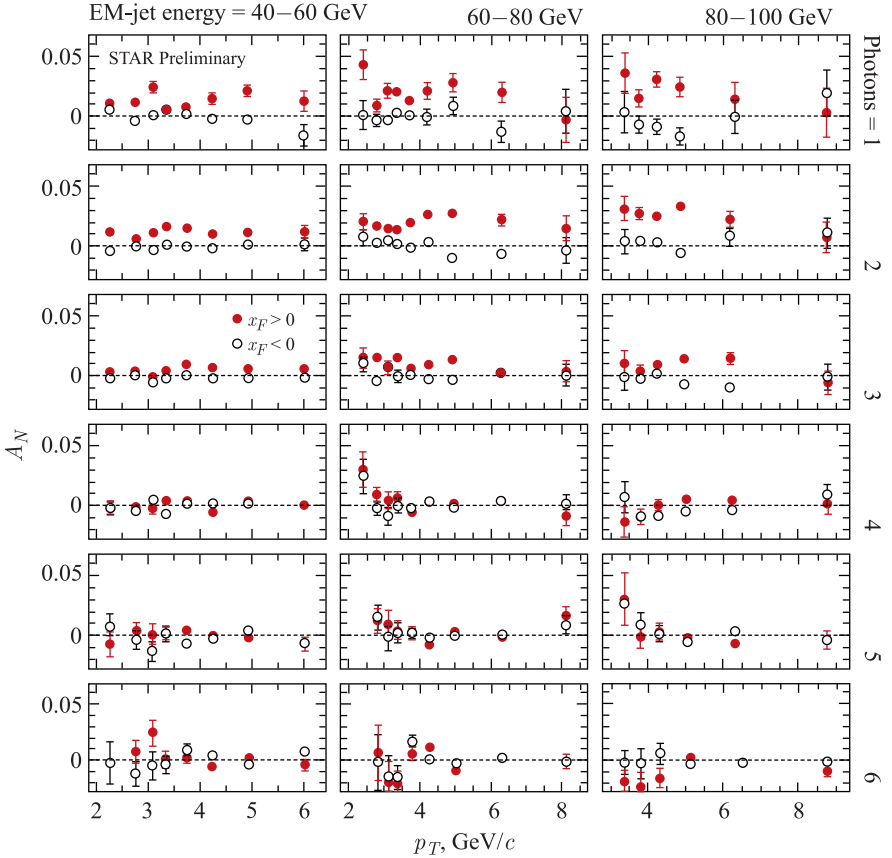

Fig. 8. The dependence of asymmetry A_N on p_T of jet produced for $x_F > 0$ and $x_F < 0$ [43]. Number of photon content in jet with different energy is shown in rows. Points are given with statistical errors only

with zero in the fragmentation range of unpolarized proton ($x_F < 0$) and for forward background.

It is assumed that the asymmetry will impose significant constraints on the contributions from the gluon Sivers function [42] and provide the much-needed input to study the energy and scale dependence for these transverse-momentum-dependent observables, which is currently under intense theoretical discussion. The observable will help to separate the contributions from initial and final states, and will give insight into the transverse spin structure of proton.

To investigate the origins of A_N, the event topology dependence of π^0 asymmetries has been studied [43]. Figure 8 demonstrates the results of analysis of the STAR data for $p^\uparrow + p$ collisions at $\sqrt{s} = 500$ GeV recorded in 2011 with 22 pb^{-1} of integrated luminosity and average beam polarization (transverse) of $(52 \pm 2)\%$. The measurements of transverse single-spin asymmetry for "electromagnetic jets" at forward rapidities $(2.5 < \eta < 4.0)$ have shown that A_N decreases with increasing number of photons in the "electromagnetic jet". It is basically flat as a function of jet p_T for all jet energies and photon multiplicities in the jet. Jets with an isolated π^0 exhibit the largest asymmetry, consistent with the asymmetry in inclusive π^0 events. This behavior is very different from naive expectations $(1/p_T)$ for an asymmetry driven by QCD subprocesses.

8. ASYMMETRY A_N OF π^0 MESON PRODUCTION IN $p^\uparrow + $ Au COLLISIONS AT $\sqrt{s} = 200$ GeV

The single-spin asymmetry, A_N, of π^0 mesons produced in $p^\uparrow + $ Au collisions may shed light on the strong interaction dynamics in nuclear collisions and to deepen our understanding of QCD in a such process. At high enough energies and low parton fraction x, the density of the gluons is so high that the saturation regime characterized by strong gluon fields is expected to be reached. The measurement of transverse spin asymmetries may provide an alternative way to study the onset of gluon saturation and quark transverse momentum distributions (TMDs) [33–35]. Some theoretical approaches based on Color Glass Condensate physics [45–49] predict that hadronic A_N should decrease with increasing size of the nuclear target. Some approaches based on perturbative QCD factorization predict that A_N would stay approximately the same for all nuclear targets (see [50] and references therein).

Figure 9 shows the transverse single-spin asymmetry, A_N, of π^0 meson production measured by STAR in forward range $2.5 < |\eta| < 4.0$ in $p^\uparrow + p$ and $p^\uparrow + $ Au collisions using Forward Meson Spectrometer (FMS) at $\sqrt{s} = 200$ GeV as a function of p_T for different mean x_F [44]. Shaded bands represent systematic uncertainty. As seen from Fig. 9, the asymmetry is nonzero for both $p^\uparrow + p$ and $p^\uparrow + $ Au collisions up to $p_T = 6$ GeV/c. Dependence of A_N on p_T and x_F demonstrates similar trends.
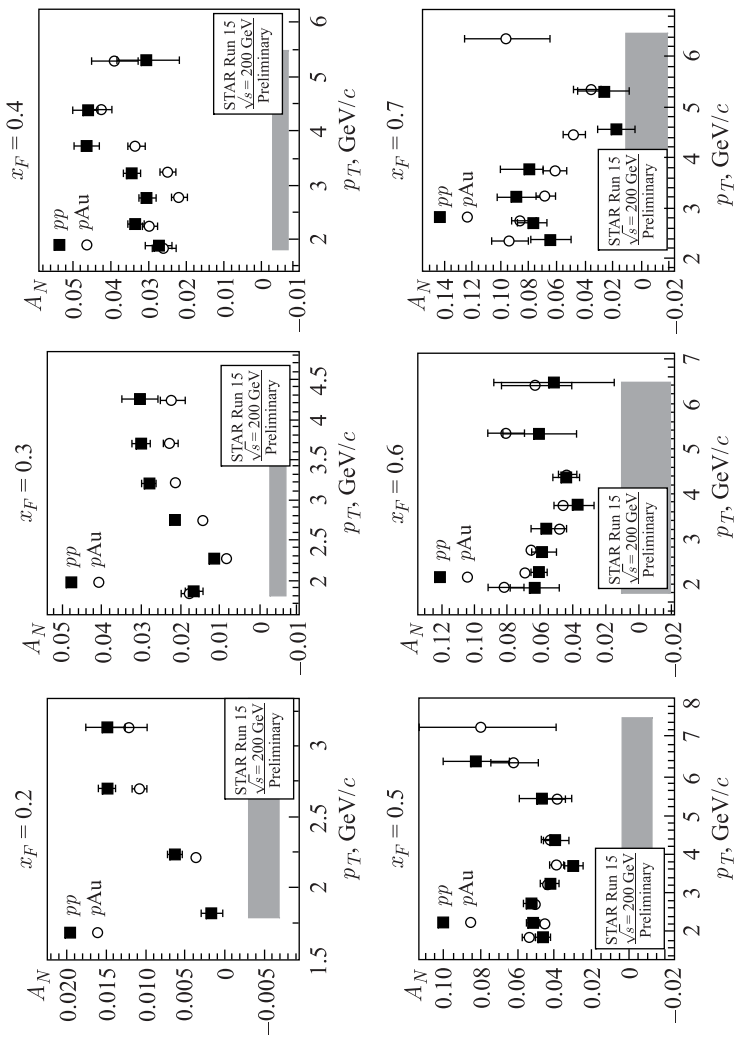
Fig. 9. The transverse single-spin asymmetry, A_N, of π^0 meson production in $p^\uparrow + p$ and $p^\uparrow + Au$ collisions at $\sqrt{s} = 200$ GeV and $2.5 < |\eta| < 4.0$ [44]

13

9. THE TRANSVERSE ASYMMETRY A_{UT} OF $\pi^{\pm}$ PAIR PRODUCTION IN $p^{\uparrow} + p$ AT $\sqrt{s} = 500$ GeV

Azimuthal transverse asymmetry A_{UT} of dipion production in polarized $p^{\uparrow} + p$ is sensitive to transversity (see [37] and references threin) and interference fragmentation function (IFF) [51]. The first observation of transverse polarization-
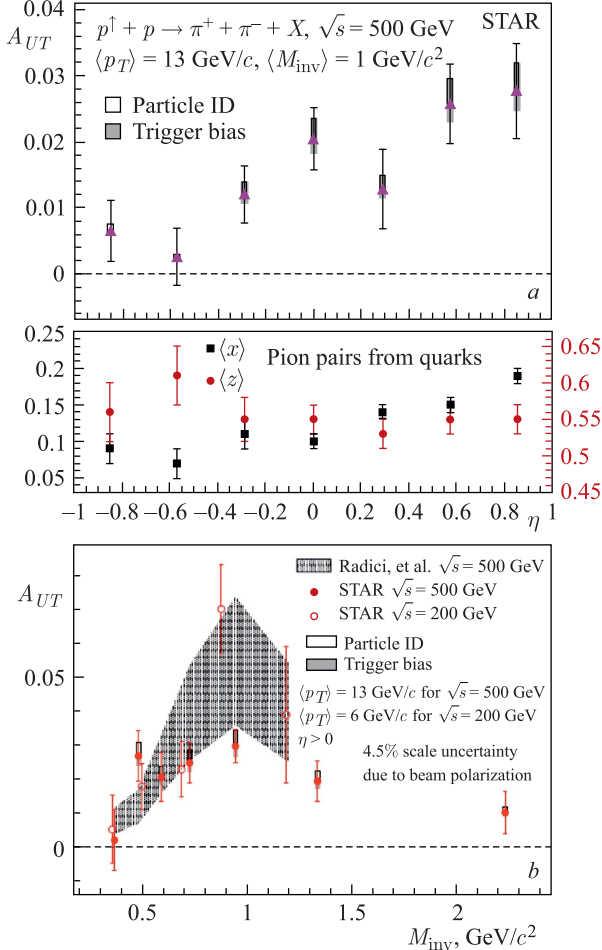

Fig. 10. *a*) The asymmetry A_{UT} and the kinematic variables, $\langle x \rangle$ and $\langle z \rangle$, plotted as a function of η for $\langle p_T \rangle = 13$ GeV/c at $\sqrt{s} = 500$ GeV. Statistical uncertainties are represented by the error bars, the open rectangles are the systematic uncertainties originating from the particle identification, and the solid rectangles represent the trigger bias systematic uncertainties. *b*) A clear enhancement of the signal around the ρ-mass region is observed at both $\sqrt{s} = 200$ and 500 GeV by STAR [52, 53]

dependent azimuthal correlations in charged pion pair production with the STAR experiment in $p^\uparrow + p$ collisions was reported in [52]. The asymmetry describes the azimuthal dependence of the correlated hadron pair on the spin of the parent quark. Such data give the possibility to extract transversity without a full global analysis. The observable is collinear and can be compared to a similar measurement in e^+e^- annihilation.

STAR has measured the first $\pi^+\pi^-$ transverse spin-dependent azimuthal asymmetries in $p^\uparrow + p$ collisions at $\sqrt{s} = 500$ GeV for several pseudorapidity, invariant mass, and transverse momentum bins [53]. These data show significant signals at high p_T and M_{inv} for $\eta > 0$. The new dataset corresponds to 25 pb^{-1} integrated luminosity collisions at $\sqrt{s} = 500$ GeV, an increase of more than a factor of ten compared to previous measurement at $\sqrt{s} = 200$ GeV [52].

Figure 10, a, shows the single-spin asymmetry, A_{UT}, as a function of η for the highest p_T with $\langle p_T \rangle = 13$ GeV/c. The other four p_T bins 4, 5, 6, and 8 GeV/c were found to have smaller asymmetries compared to the highest $\langle p_T \rangle$. As seen in Fig. 10, a, a strong rise of the measured signal is observed toward higher η as x increases. This is consistent with the expectation that the transversity distribution is suppressed at low x. The bottom panel shows $\langle x \rangle$ and $\langle z \rangle$ as a function of pion pair pseudorapidity. Figure 10, b, demonstrates the dependence of A_{UT} on invariant mass M_{inv} of $\pi^+\pi^-$ pair for the highest $\langle p_T \rangle = 6$ GeV/c at $\sqrt{s} = 200$ GeV and 13 GeV/c at 500 GeV for $\eta_{\pi^+\pi^-} > 0$. As seen from Fig. 10, b, the data show an enhancement of the asymmetry around the ρ mass. The effect is related with the interference of vector meson decays in a relative p-wave with the non-resonant background in a relative s-wave. The gray band represents the range of the 68% confidence interval of the fit to SIDIS and e^+e^- data. The calculation (as prediction) was done by the authors of reference [54] at energy $\sqrt{s} = 200$ GeV and then compared to the results from [52].

10. THE TRANSVERSE AZIMUTHAL ASYMMETRY A_{UT} OF jet $+ \pi^\pm$ PRODUCTION IN $p^\uparrow + p$ AT $\sqrt{s} = 500$ GeV

Azimuthal distributions of hadrons inside large transverse-momentum jets in transversely polarized proton–proton collisions are a very important and complementary source of information on TMD distribution and fragmentation functions and provide a unique tool to constrain transversity distributions [55, 56]. Sinusoidal modulations in particle production can be measured with respect to two azimuthal angles: ϕ_S, the azimuthal angle between the proton transverse spin polarization vector and the jet scattering plane, and ϕ_H, the azimuthal angle of the pion relative to the jet scattering plane. The $\sin(\phi_S - \phi_H)$ modulation of A_{UT} yields sensitivity to transversity coupled to the polarized Collins fragmentation function. The first observation of Collins A_{UT} asymmetries in $p^\uparrow + p$ collisions at $\sqrt{s} = 200$ GeV was reported in [57].
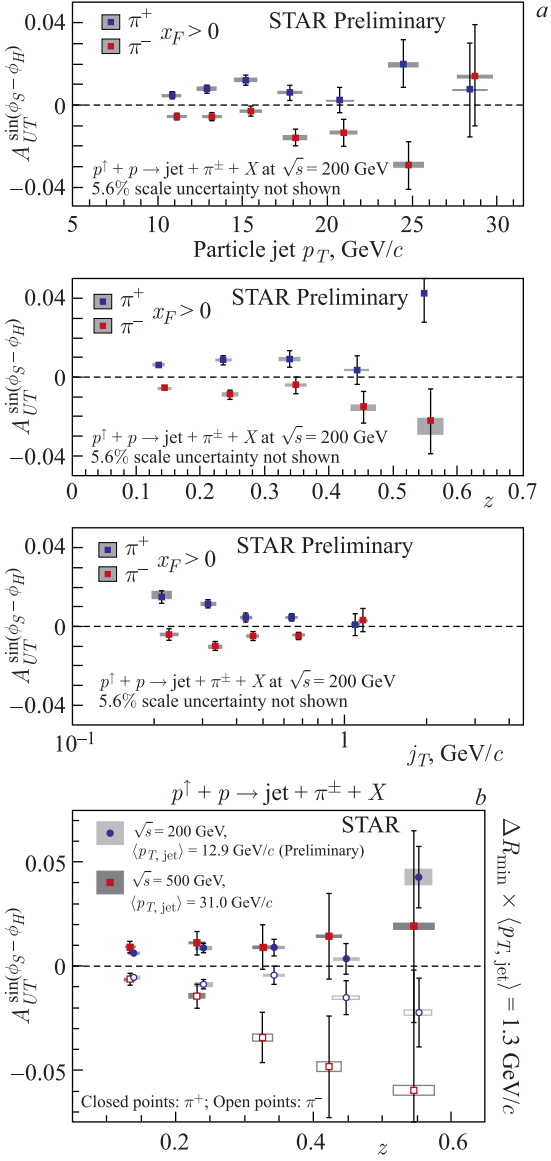
Fig. 11. The azimuthal asymmetry A_{UT} of jet $+ \pi^{\pm}$ production in transversely polarized $p^{\uparrow} + p$ collisions as a function of jet transverse momentum, $z = p_{\pi}/p_{\text{jet}}$ and transverse momentum (j_T) for charged pions in jets for $0 < \eta < 1$ at $\sqrt{s} = 200$ (a), and as a function of z at 500 GeV (b) measured by STAR [57, 58]

16

The first measurements of transverse single-spin asymmetries from inclusive jet + $\pi^{\pm}$ production in the central pseudorapidity range from $p^{\uparrow} + p$ at $\sqrt{s} = 500$ GeV are reported in [58]. The data were collected in 2011 with the STAR detector sampled from 23 pb^{-1} integrated luminosity with an average beam polarization of 53%.

Figure 11 shows the first clear observations of nonzero Collins asymmetries in proton–proton collisions at $\sqrt{s} = 200$ (*a*) and 500 GeV (*b*) by STAR [57, 58]. STAR found that the azimuthal transverse asymmetry of pions in polarized jet production depends strongly on momentum j_T of the pion transverse to the jet thrust axis. Large asymmetries are seen from Fig. 11, *a*, for moderate values of j_T, whereas much smaller asymmetries are found when the measurement is restricted to larger values of j_T. Note that the nonzero Collins asymmetries in polarized-proton collisions at high values of jet transverse momenta are observed. A statistical significance was found to be greater than 5σ. As seen from Fig. 11, *b*, the asymmetry for π^{+} mesons is found to be positive, while that for π^{-} mesons is negative. The results are consistent with the expectation for TMD factorization in proton–proton collisions and universality of the Collins fragmentation function. The data show a slight preference for models assuming no suppression from TMD evolution.

11. TRANSVERSE SPIN TRANSFER COEFFICIENT D_{TT} IN $p^{\uparrow} + p$ AT $\sqrt{s} = 200$ GeV

Transverse spin transfer from polarized proton to polarized Λ and $\bar{\Lambda}$ provides insights into transversely polarized fragmentation and transversity distribution functions [59, 60]. The transversely polarized cross section for the process $p^{\uparrow} + p \rightarrow \Lambda^{\uparrow} + X$ can be factorized into the convolution of the transversity distribution function, the transversely polarized partonic cross section and the transversely polarized fragmentation function.

Significant spin transfer has been found at large $x_F \simeq 0.8$ with a 200 GeV/c transversely polarized proton beam in fixed target experiment at FNAL [61].

The transverse spin transfer is defined as

$$D_{TT} = \frac{\sigma^{p^{\uparrow}p \rightarrow \Lambda^{\uparrow}X} - \sigma^{p^{\uparrow}p \rightarrow \Lambda^{\downarrow}X}}{\sigma^{p^{\uparrow}p \rightarrow \Lambda^{\uparrow}X} + \sigma^{p^{\uparrow}p \rightarrow \Lambda^{\downarrow}X}}. \qquad (4)$$

The polarization of Λ and $\bar{\Lambda}$ is extracted from the angular distribution of its decay product in its rest frame.

Figure 12 shows the first STAR measurement of transverse spin transfer D_{TT} of Λ and $\bar{\Lambda}$ in $p^{\uparrow} + p$ collision at $\sqrt{s} = 200$ GeV and $\eta > 0$ (*a*), $\eta < 0$ (*b*) as a function of transverse momentum p_T [62]. The analysis is based on data sample taken with STAR detector in 2012 for transversely polarized $p^{\uparrow} + p$ collisions.
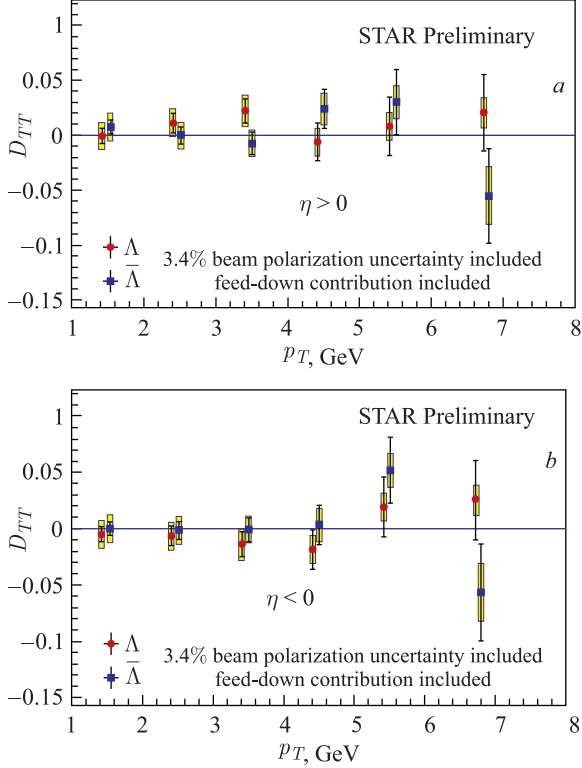
Fig. 12. Transverse spin transfer D_{TT} of Λ and $\bar{\Lambda}$ in transversely polarized proton–proton collisions at $\sqrt{s} = 200$ GeV [62] for $\eta > 0$ (*a*) and $\eta < 0$ (*b*)

We note that this is the most precise measurement on Λ and $\bar{\Lambda}$ polarization in $p^{\uparrow} + p$ collisions at RHIC with a statistical uncertainty of 0.04 at $p_T \simeq 7$ GeV/*c*. The dominant source of systematic uncertainty is from relative luminosity in low p_T. As seen from Fig. 12, D_{TT} values of Λ and $\bar{\Lambda}$ are consistent with each other and consistent with zero at the presently available precision.

12. STAR FORWARD UPGRADE

The STAR forward upgrade [63] will enable STAR to investigate the full physics program outlined in the RHIC Cold QCD Plan [64]. STAR proposes to include new subsystems — the Forward Calorimeter System (FCS) and the Forward Tracking System (FTS), with superior detection capability for neutral pions, photons, electrons, jets and charged hadrons covering a pseudorapidity region of $2.5 < \eta < 4.5$. The FCS will utilize the existing Forward Preshower Detector that has been operated successfully in STAR since 2015. The proposed FCS system

will have very good ($\sim 8\%/\sqrt{E}$) electromagnetic and ($\sim 70\%/\sqrt{E}$) hadronic energy resolutions. A Forward Tracking System needs to be designed for the small field-integral from the STAR 0.5 T solenoid magnet field in the forward region to discriminate charge sign for transverse asymmetry studies and those of electrons and positrons for Drell–Yan measurements. It needs to find primary vertices for tracks and point them towards the calorimeters in order to suppress pile-up events in the anticipated high-luminosity collisions, or to select particles from Λ decays. It should also help with electron and photon identification by providing momentum and track veto information. In order to keep multiple scattering and photon conversion background under control, the material budget of the FTS has to be small. The proposed FTS is designed to meet the detector requirements for position resolution, fast readout, high efficiency, and low material budget.

13. SUMMARY

Recent STAR spin results on the double longitudinal asymmetry, A_{LL}, of pion and jet production at $\sqrt{s} = 200$ and 510 GeV, the single longitudinal, A_L, and transverse, A_N, asymmetry of $W^{\pm}$ production at $\sqrt{s} = 510$ GeV and STAR forward upgrade are briefly overviewed. We would like to note that

• RHIC remains the only polarized high-energy proton collider in the world;

• Large and uniform acceptance, excellent PID of the STAR experiment allow us to perform measurements with unpolarized, longitudinally and transversely polarized protons up to $\sqrt{s} = 510$ GeV;

• The inclusion of STAR data into global PDF and FF analyses helps to determine the gluon polarization contribution to proton spin, helicity of sea quarks and to understand the origin of transverse spin asymmetry;

• The forward upgrade at STAR with FCS and FTS would significantly improve the capabilities of the STAR experiment for measurements of observables such as asymmetries of pion, jet, Drell–Yan e^+e^- pairs produced at forward rapidity in $p^{\uparrow} + p$ and $p^{\uparrow} + A$ collisions;

• The upgrade program will enable us to study the longitudinal structure of the proton, the breaking of boost invariance in heavy-ion collisions, to explore the transport properties of the hot and dense matter formed in heavy-ion collisions near the region of perfect fluidity;

• Measurements planned to be performed by STAR will be complementary and necessary for a smooth transition toward the physics program at a future Electron Ion Collider [65].

REFERENCES

1. *Harrison M., Ludlam T., Ozaki S.* The Relativistic Heavy Ion Collider Project: RHIC and Its Detectors // Nucl. Instrum. Meth. A. 2003. V. 499(2–3). P. 235–880.
2. *Alekseev I. et al.* Polarized Proton Collider at RHIC // Nucl. Instrum. Meth. A. 2003. V. 499. P. 392–414.

3. *Zelenski A. et al.* Optically Pumped Polarized H$^-$ Ion Source for RHIC Spin Physics // Rev. Sci. Instrum. 2002. V. 73. P. 888.

4. *Derbenev Ya. S. et al.* Radiative Polarization: Obtaining, Control, Using // Part. Accel. 1978. V. 8. P. 115–126.

5. *Nakagawa I. et al.* p-Carbon Polarimetry at RHIC // AIP Conf. Proc. 2008. V. 980. P. 380–389.

6. *Zelenski A. et al.* Absolute Polarized H$^-$ Jet Polarimeter Development for RHIC // Nucl. Instrum. Meth. A. 2005. V. 536. P. 248–254.

7. *MacKay W. W. et al.* Commissioning Spin Rotators in RHIC // Proc. IEEE Particle Accelerator Conference, New York, 2003 / Ed. by J. Chew, P. Lucas and S. Webber. P. 1697–1699.

8. *Ackermann K. H. et al. (STAR Collab.).* STAR Detector Overview // Nucl. Instrum. Meth. A. 2003. V. 499. P. 624–632.

9. *Anderson M. et al. (STAR Collab.).* The STAR Time Projection Chamber: A Unique Tool for Studying High Multiplicity Events at RHIC // Nucl. Instrum. Meth. A. 2003. V. 499. P. 659–678.

10. *Llope W. et al. (STAR Collab.).* The Large-Area Time-of-Flight Upgrade for STAR // Nucl. Instrum. Meth. B. 2005. V. 241. P. 306–310.

11. *Geurts F. et al.* Performance of the Prototype MRPC Detector for STAR // Nucl. Instrum. Meth. A. 2004. V. 533. P. 60–64.

12. *Wang Y. et al.* Production and Quality Control of STAR-TOF MRPC // Nucl. Instrum. Meth. A. 2010. V. 613. P. 200–206.

13. *Beddo M. et al. (STAR Collab.).* The STAR Barrel Electromagnetic Calorimeter // Nucl. Instrum. Meth. A. 2003. V. 499. P. 725–739.

14. *Allgower C. E. et al. (STAR Collab.).* The STAR Endcap Electromagnetic Calorimeter // Nucl. Instrum. Meth. A. 2003. V. 499. P. 740–750.

15. *Adamczyk L. et al. (STAR Collab.).* Longitudinal and Transverse Spin Asymmetries for Inclusive Jet Production at Mid-Rapidity in Polarized $p + p$ Collisions at $\sqrt{s} = 200$ GeV // Phys. Rev. D. 2012. V. 86. P. 032006.

16. *Kiryluk J. (for the STAR Collab.).* Local Polarimetry for Proton Beams with the STAR Beam Beam Counters. https://arxiv.org/abs/hep-ex/0501072.

17. *Ackermann K. H. et al. (STAR Collab.).* STAR Detector Overview // Nucl. Instrum. Meth. A. 2003. V. 499. P. 624–632.

18. *Llope W. J. et al. (STAR Collab.).* The STAR Vertex Position Detector // Nucl. Instrum. Meth. A. 2014. V. 759. P. 23–28.

19. *Adamczyk L. et al. (STAR Collab.).* Precision Measurement of the Longitudinal Double-Spin Asymmetry for Inclusive Jet Production in Polarized Proton Collisions at $\sqrt{s} = 200$ GeV // Phys. Rev. Lett. 2015. V. 115. P. 092002.

20. *Gagliardi C. (for STAR Collab.).* Probing the Origin of the Proton Spin at STAR // ICNFP2017, Kolymbari, Greece, Aug. 17–26, 2017; https://indico.cern.ch/event/559774/overview.

21. *Nocera E. R., Ball R. D., Forte S., Ridolfi G., Rojo J.* A First Unbiased Global Determination of Polarized PDFs and Their Uncertainties // Nucl. Phys. B. 2014. V. 887. P. 276–308.

22. *Adamczyk L. et al. (STAR Collab.).* Measurement of the Cross Section and Longitudinal Double-Spin Asymmetry for Di-Jet Production in Polarized pp Collisions at $\sqrt{s} = 200$ GeV // Phys. Rev. D. 2017. V. 95. P. 071103.

23. *de Florian D., Frixione S., Signer A., Vogelsang W.* Next-to-Leading Order Jet Cross Sections in Polarized Hadronic Collisions // Nucl. Phys. B. 1999. V. 539. P. 455–476.

24. *Lai H. L. et al.* New Parton Distributions for Collider Physics // Phys. Rev. D. 2010. V. 82. P. 074024.

25. *de Florian D., Sassot R., Stratmann M., Vogelsang W.* Evidence for Polarization of Gluons in the Proton // Phys. Rev. Lett. 2014. V. 113. P. 012001.

26. *Adamczyk L. et al. (STAR Collab.).* Measurement of Longitudinal Spin Asymmetries for Weak Boson Production in Polarized Proton–Proton Collisions at RHIC // Phys. Rev. Lett. 2014. V. 113. P. 072301.

27. *de Florian D., Vogelsang W.* Helicity Parton Distributions from Spin Asymmetries in W-Boson Production at RHIC // Phys. Rev. D. 2010. V. 81. P. 094020.

28. *Gunarathne D. (for the STAR collab.).* Measurement of $W^{\pm}$ Single Spin Asymmetries and W Cross Section Ratio in Polarized $p+p$ Collisions at $\sqrt{s} = 510$ GeV at STAR. https://arxiv.org/abs/1702.02927.

29. *Adamczyk L. et al. (STAR Collab.).* Measurement of the Transverse Single-Spin Asymmetry in $p^{\uparrow} + p \to W^{\pm}/Z^0$ at RHIC // Phys. Rev. Lett. 2016. V. 116. P. 132301.

30. *Sivers D. W.* Single-Spin Production Asymmetries from the Hard Scattering of Point-like Constituents // Phys. Rev. D. 1990. V. 41. P. 83–90.

31. *Sivers D. W.* Hard Scattering Scaling Laws for Single Spin Production Asymmetries // Phys. Rev. D. 1991. V. 43. P. 261–263.

32. *Kang Z.-B., Qiu J.-W.* Testing the Time-Reversal Modified Universality of the Sivers Function // Phys. Rev. Lett. 2009. V. 103. P. 172001.

33. *Aybat S. M., Prokudin A., Rogers T. C.* Calculation of Transverse-Momentum-Dependent Evolution for Sivers Transverse Single Spin Asymmetry Measurements // Phys. Rev. Lett. 2012. V. 108. P. 242003.

34. *Anselmino M., Boglione M., Melis S.* Strategy Towards the Extraction of the Sivers Function with Transverse Momentum Dependent Evolution // Phys. Rev. D. 2012. V. 86. P. 014028.

35. *Sun P., Yuan F.* Transverse Momentum Dependent Evolution: Matching Semi-Inclusive Deep Inelastic Scattering Processes to Drell–Yan and W/Z Boson Production // Phys. Rev. D. 2013. V. 88. P. 114012.

36. *Aidala Ch. A. et al.* The Spin Structure of the Nucleon // Rev. Mod. Phys. 2013. V. 85. P. 655–691.

37. *Barone V., Bradamante F., Martin A.* Transverse-Spin and Transverse-Momentum Effects in High-Energy Processes // Prog. Part. Nucl. Phys. 2010. V. 65. P. 267–333.

38. *Pan Y. (for STAR Collab.).* Transverse Single Spin Asymmetries of Forward π^0 and Jet-Like Events in $\sqrt{s} = 500$ GeV Polarized Proton Collisions at STAR // Int. J. Mod. Phys.: Conf. Ser. 2016. V. 40. P. 1660037.

39. *Adams D. L. et al. (E581 and E704 Collabs.).* Comparison of Spin Asymmetries and Cross-Sections in π^0 Production by 200-GeV Polarized Anti-Protons and Protons // Phys. Lett. B. 1991. V. 261. P. 201–206.

40. *Adams D. L. et al. (E704 Collab.).* Analyzing Power in Inclusive π^+ and π^- Production at High $x(F)$ with a 200-GeV Polarized Proton Beam // Phys. Lett. B. 1991. V. 264. P. 462–466.

41. *Adamczyk L. et al. (STAR Collab.).* Neutral Pion Cross Section and Spin Asymmetries at Intermediate Pseudorapidity in Polarized Proton Collisions at $\sqrt{s} = 200$ GeV // Phys. Rev. D. 2014. V. 89. P. 012001.

42. *D'Alesio U., Murgia F., Pisano C., Taels P.* Probing the Gluon Sivers Function in $p^\uparrow p \to J/\psi X$ and $p^\uparrow p \to D X$ // Phys. Rev. D. 2017. V. 96. P. 036011.

43. *Mondal M. M. (for STAR Collab.).* Measurement of the Transverse Single-Spin Asymmetries for π^0 and Jet-Like Events at Forward Rapidities at STAR in $p + p$ Collisions at $\sqrt{s} = 500$ GeV. https://arxiv.org/abs/1407.3715.

44. *Heppelman S. (for STAR Collab.).* Preview from RHIC Run 15 pp and pAu Forward Neutral Pion Production from Transversely Polarized Protons // 7th Int. Workshop on Multiple Partonic Interactions at the LHC "MPI@LHC", Trieste, Italy, November 23–27, 2015. P. 228–231.

45. *Boer D., Dumitru A., Hayashigaki A.* Single Transverse-Spin Asymmetries in Forward Pion Production at High Energy: Incorporating Small-x Effects in the Target // Phys. Rev. D. 2006. V. 74. P. 074018.

46. *Boer D., Dumitru A.* Polarized Hyperons from pA Scattering in the Gluon Saturation Regime // Phys. Lett. B. 2003. V. 556. P. 33–40.

47. *Boer D., Utermann A., Wessels E.* The Saturation Scale and Its x-Dependence from Lambda Polarization Studies // Phys. Lett. B. 2009. V. 671. P. 91–98.

48. *Kang Z.-B., Yuan F.* Single Spin Asymmetry Scaling in the Forward Rapidity Region at RHIC // Phys. Rev. D. 2011. V. 84. P. 034019.

49. *Kovchegov Y. V., Sievert M. D.* A New Mechanism for Generating a Single Transverse Spin Asymmetry // Phys. Rev. D. 2012. V. 86. P. 034028; Erratum // 2012. Phys. Rev. D. V. 86. P. 079906.

50. *Aschenauer E. C. et al.* The RHIC SPIN Program: Achievements and Future Opportunities. https://arxiv.org/abs/1304.0079.

51. *Pisano S., Radici M.* Di-Hadron Fragmentation and Mapping of the Nucleon Structure // Eur. Phys. J. A. 2016. V. 52. P. 155.

52. *Adamczyk L. et al. (STAR Collab.).* Observation of Transverse Spin-Dependent Azimuthal Correlations of Charged Pion Pairs in $p^\uparrow + p$ at $\sqrt{s} = 200$ GeV // Phys. Rev. Lett. 2015. V. 115. P. 242501.

53. *Adamczyk L. et al. (STAR Collab.).* Transverse Spin-Dependent Azimuthal Correlations of Charged Pion Pairs Measured in $p^\uparrow + p$ Collisions at $\sqrt{s} = 500$ GeV. https://arxiv.org/abs/1710.10215.

54. *Radici M., Ricci A. M., Bacchetta A., Mukherjee A.* Exploring Universality of Transversity in Proton–Proton Collisions // Phys. Rev. D. 2016. V. 94. P. 034012.

55. *D'Alesio U., Murgia F., Pisano C.* Azimuthal Asymmetries for Hadron Distributions inside a Jet in Hadronic Collisions // Phys. Rev. D. 2011. V. 83. P. 034021.

56. *Yuan F.* Asymmetric Azimuthal Distribution of Hadrons inside a Jet from Hadron–Hadron Collisions // Phys. Rev. Lett. 2008. V. 100. P. 032003.

57. *Adkins J. K., Drachenberg J. L. (for STAR Collab.).* Azimuthal Single-Spin Asymmetries of Charged Pions in Jets in $\sqrt{s} = 200$ GeV $p^{\uparrow}p$ Collisions at STAR // Int. J. Mod. Phys.: Conf. Ser. 2016. V. 40. P. 1660040.

58. *Adamczyk L. et al. (STAR Collab.).* Azimuthal Transverse Single-Spin Asymmetries of Inclusive Jets and Charged Pions within Jets from Polarized-Proton Collisions at $\sqrt{s} = 500$ GeV // Phys. Rev. D. 2018. V. 97. P. 032004.

59. *Xu Q., Liang Z., Sichterman E.* Anti-Lambda Polarization in High Energy pp Collisions with Polarized Beam // Phys. Rev. D. 2006. V. 73. P. 077503.

60. *de Florian D., Soffer J., Stratmann M., Vogelsang W.* Bounds on Transverse Spin Asymmetries for Λ Baryon Production in pp Collisions at BNL RHIC // Phys. Lett. B. 1998. V. 439. P. 176–182.

61. *Bravar A. et al. (Fermilab E704 Collab.).* Spin Transfer in Inclusive Λ^0 Production by Transversely Polarized Protons at 200 GeV/c // Phys. Rev. Lett. 1997. V. 78. P. 4003–4006.

62. *Mei J. (for STAR Collab.).* Measurement of Transverse Spin Transfer of Lambda and Anti-Lambda Hyperons in Polarized Proton+Proton Collisions at STAR // PoS DIS2017. 2018. P. 225.

63. *STAR Collab.* The STAR Forward Calorimeter System and Forward Tracking System. https://drupal.star.bnl.gov/STAR/starnotes/public/sn0648.

64. *Aschenauer E. C. et al.* The RHIC Cold QCD Plan for 2017 to 2023: A Portal to EIC. https://arxiv.org/abs/1602.03922.

65. *Accardi A. et al.* Electron Ion Collider: The Next QCD Frontier — Understanding the Glue That Binds Us All. https://arxiv.org/abs/1212.1701.